

Enforcing Label and Intensity Consistency for IR Target Detection*

Toufiq Parag

Janelia Farm Research Campus-HHMI, Ashburn, VA 20147

Abstract

This study formulates the IR target detection as a binary classification problem of each pixel. Each pixel is associated with a label which indicates whether it is a target or background pixel. The optimal label set for all the pixels of an image maximizes a posteriori distribution of label configuration given the pixel intensities. The posterior probability is factored into (or proportional to) a conditional likelihood of the intensity values and a prior probability of label configuration. Each of these two probabilities are computed assuming a Markov Random Field (MRF) on both pixel intensities and their labels. In particular, this study enforces neighborhood dependency on both intensity values, by a Simultaneous Auto Regressive (SAR) model, and on labels, by an Auto-Logistic model. The parameters of these MRF models are learned from labeled examples. During testing, an MRF inference technique, namely Iterated Conditional Mode (ICM), produces the optimal label for each pixel. The detection performance is further improved by incorporating temporal information through background subtraction. High performances on benchmark datasets demonstrate effectiveness of this method for IR target detection.

1 Introduction

Infrared (IR) images provide valuable information for visual surveillance. Since IR wavelength responds to heat, it can indicate the locations of objects

*First appeared in OTCBVS 2011 [16]. This manuscript presents updated results and an extension.

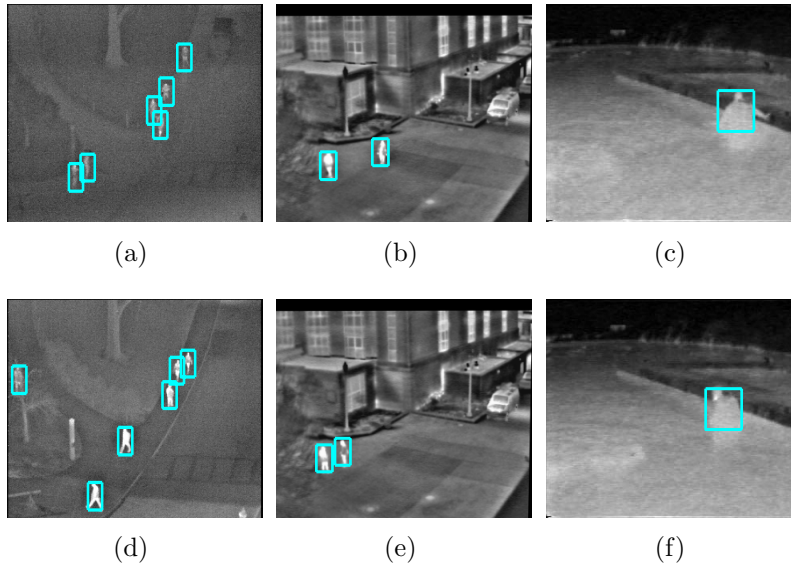


Figure 1: Sample input images for IR target detection.

in an image taken during the day or at night. Hence, these images can be exploited in surveillance system that need to be executed around the clock or in scenarios where visual features are not discriminative enough for detection. But, detecting objects in IR images is not trivial. Targets are often not as illuminated as one would expect in ideal case. To deteriorate the situation, luminous background regions also appear frequently in thermal images. We show several sample images in Figure 1 where (groundtruth) target locations are displayed in rectangles.

The images (a) and (d) in Figure 1 indicate that the distribution pixel intensities within target region is multimodal. Comparing these images with (b) and (e), one could realize that the distribution also overlaps with that of background pixel values. The overlap is even more evident in images (c) and (f) that show a swimmer/diver swimming coming out of the water. These images strongly suggest that the same object detector can not work satisfactorily for all these scenarios – we need to learn the object pattern for each of these cases. Furthermore, it is also evident that independently pixel intensities are not discriminative features for target classification. These characteristics are also observed by past studies which uses different other

low level features as described in the next paragraph. It is worth noting that, though the individual pixel values are not very discriminative, intensity arrangement within an image patch seems to be highly informative and could potentially result in superior performance if modeled appropriately.

Detecting pedestrians in natural images (i.e., visible spectrum) has gained much attention in past several years [3][22][6]. Several previous works on IR object detection extended algorithms for pedestrian detection in visible spectrum to thermal images. The study by Zhang et. al. [25] experimented with the Edgelet and Histogram of Oriented Gradient (HOG) and applied Adaboost and Support Vector Machine (SVM) classifiers to identify pedestrian in IR images. The work in [10] uses the SURF features and utilizes a voting scheme of detected codewords to determine object location in image. A more recent work [21] computes composite combinatorial features from low level features such as intensities and HOG to represent object pattern and employs a boosting classifier for detection. Though these studies indirectly learn the pattern of object patch (as described by the features they use), they do not explicitly model the relationship of the pixel values and their labels with neighboring ones. More specifically, the labels of the pixels are considered to be independent of each other.

Other approach such as [7] proposes a method to refine the contours of foreground regions, detected by a background subtraction model, to determine the target locations. Temporal information between consecutive frames, is utilized in IR object detection as well. Wang et. al. [23] combines the results of detection and tracking to extract target locations from scene. Temporal information is shown to assist identifying small objects and to remove many false positive locations otherwise detected in single frame methods. In [12], the authors combines thermal and visible information and adopt a Particle Filtering approach for tracking (multiple) people in the image. An earlier work [5] of similar spirit adds shape information with appearance to identify objects foreground regions.

This paper proposes to model both the pixel intensities and labels to be dependent upon those of its neighbors. The optimal label configuration of image pixels is supposed to maximize the posterior probability given the intensity configuration. This posterior can be factored to a conditional likelihood of intensity configuration and a prior probability of the label configuration. We model both the conditional likelihood of intensity arrangement (given the label arrangement) and prior probability of labels using (two different types of) Markov Random Field (MRF) [13]. As a result, both the label and inten-

sity of a pixel becomes related to those of its neighbors. This relationship is learned from given examples of target and background patches. Intuitively, we are learning the intensity and label correlation patterns in target regions of IR images. An MRF inference algorithm, namely the Iterated Conditional Modes (ICM), determine the optimal value of pixel labels during test phase.

In a similar spirit of [7, 23], we also combine temporal information in order to refine the detection performance. The result of a background subtraction algorithm is fused with that of the proposed method to generate the final detection output. Background subtraction and change detection techniques have a relatively longer history than other low level vision problems in computer vision literature, see [15] and the references therein. Most of these studies represent the temporal history of background pixel intensities by a parametric or non-parametric statistical model; pixel locations whose intensity significantly deviates from this model are classified as foreground pixels. Although the background subtraction method alone can not produce a satisfactory performance [7], we show that they can assist the proposed method to achieve the maximal hit rate with zero false detections.

Since its introduction, MRF models have been applied to many problems in vision. Due to recent discoveries of elegant and efficient inference algorithms, MRF models have become widely popular in vision. Some notable applications are image segmentation [4][18], object recognition [11], stereo matching, feature correspondence [20], image denoising and reconstruction [17], clustering [24] etc. Surprisingly enough, MRF has not yet been used for IR target detection to the best of our knowledge.

Coupled MRF models were also used in [8] and [19] for texture segmentation of images. We show the applicability of similar framework on IR images for target detection. The specific instances of MRF models assumed in these studies are different from those incorporated in this paper. There exist more sophisticated frameworks that represent the pixel intensity arrangement within a patch by MRF models, e.g., [14] or more recent Fields of Expert model [17].

The paper is organized as follows: Section 2 describes the overall probability structure followed by our method. Section 3 describes the specific MRFs imposed on intensity and label layers. Techniques for learning the parameter values and for computing the optimal labels of test images are discussed in Sections 4 and 5 respectively. We report the results of our method on benchmark datasets in Section 7 before concluding our findings in Section 8.

2 MAP Estimation of Target Locations

Let $\mathbf{y} = \{y_i \in \mathbb{R} \mid i = 1, \dots, n\}$ be the intensities of an IR image. We wish to label each location i in the image to be a background or target pixel. Let $\mathbf{x} = \{x_i \in \{0, 1\} \mid i = 1, \dots, n\}$ be the class labels for pixels in this image : $x_i = 1$ and 0 implies a target and background pixel respectively. Then, our goal is to compute the optimal label configuration \mathbf{x}^* that maximizes the aposteriori distribution $p(\mathbf{x} \mid \mathbf{y}) \propto p(\mathbf{y} \mid \mathbf{x}) p(\mathbf{x})$. In the proposed framework, both the conditional likelihood $p(\mathbf{y} \mid \mathbf{x})$ and the prior $p(\mathbf{x})$ are modeled by Markov Random Field (MRF)s. Our objective is to compute the optimal values of both \mathbf{y} and \mathbf{x} provided the intra-layer relationship (captured by respective MRFs) and the inter-layer dependence utilizing appropriate stactical inference techniques. The probabilistic dependencies among the intensities, class labels and in between are depicted in Figure 2.

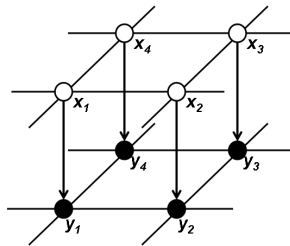


Figure 2: Bi-layer MRF model.

3 MRF Models for Target Detection

Markov Random Field (MRF) is a probabilistic graphical structure designed to model the dependence among (neighboring) datapoints. In MRF, a random variable is considered to be probabilistically dependent only to its neighbors. There are several different definitions of neighborhood systems, for example, a pixel in an image is a neighbor of all other pixels it is connected to in 4-connectivity. A pairwise (or higher order) relation among the neighbors is defined as clique within a neighborhood. Given a suitable definition of neighborhood and clique, the joint probability of a set of variables ω is given

by

$$p(\boldsymbol{\omega}) = \frac{1}{Z} \exp\left\{-\sum_{c \in \mathcal{C}} E_c(\boldsymbol{\omega}_c)\right\}, \quad (1)$$

where Z is a normalizing term [13]. The set of variables may either correspond to the class labels \mathbf{x} or to the intensity levels \mathbf{y} (conditional on \mathbf{x}). For each clique c in the set \mathcal{C} of all possible cliques, a cost (or potential) function E_c penalizes the disagreement among the values of $\boldsymbol{\omega}_c$ associated with c . The optimal $\boldsymbol{\omega}^*$ is the one that maximizes the joint probability, or, in other words, minimizes the so called Gibbs energy function $E(\boldsymbol{\omega}) = \sum_{c \in \mathcal{C}} E_c(\boldsymbol{\omega}_c)$. Definition of neighborhood and clique varies with application, e.g., considering the pixel arrangement in an image as a grid, a 4-connectivity defines a first order neighborhood and all possible pairs containing the reference variable are defined as cliques [13].

We use a functionally homogenous potential function, that is $E_c = E$ for all $c \in \mathcal{C}$. Following two sections discuss the MRF models for the conditional likelihood and prior distribution respectively.

3.1 MRF for Conditional Likelihood

We model the conditional probability $p(\mathbf{y}|\mathbf{x})$ of intensities at all pixel locations by an MRF. That is, our model imposes a dependence among intensity y_i at each pixel to those y_j , $j \in \mathcal{N}_i$, in the neighborhood \mathcal{N}_i of pixel i . The conditional likelihood $p(\mathbf{y} | \mathbf{x})$ is factored into locally dependent probabilities by assuming a Simultaneous Auto Regression (SAR) MRF over the intensities. Essentially, we are assuming that the pixel intensity of any specific location is dependent to those of its neighboring locations. In SAR model, the deviation between intensity at location i and its mean is expressed by linear combination of the deviations of its neighboring pixels perturbed by Gaussian noise. It should be clarified here that, the pattern of interaction among the neighboring pixels will be different for the target and background class. Therefore, in order to represent the neighborhood relationship, we need two SAR MRFs: one for the target and the other for the background class.

In our framework, we assume all the pixels of a particular class $l \in \{\text{target, background}\}$ are generated from same process with mean μ^l . The noise variance is also assumed to the same $(\sigma^l)^2$ for each class. The pixel value y_i at location i is related to its neighbors in SAR model for class

$l \in \{\text{object, background}\}$ by the following equation.

$$y_i = \mu^l + \sum_{j \in \mathcal{N}_i} \beta_{ij}^l (y_j - \mu^l) + \epsilon. \quad (2)$$

The parameters β_{ij}^l determines the influence of the neighboring pixels $j \in \mathcal{N}_i$ on pixel i . The value of β_{ij}^l will be different for different j , i.e., different neighbor locations within the neighborhood. The noise is assumed to be Gaussian with zero mean and standard deviation σ^l . The conditional probability of y_i given only its neighbors, which will be useful in computing MRF inference, is therefore follows a Normal distribution with mean $\mu^l + \sum_{j \in \mathcal{N}_i} \beta_{ij}^l (y_j - \mu^l)$ and variance $(\sigma^l)^2$

$$p(y_i | x_i = l, y_{\mathcal{N}_i}) = \frac{1}{(2\pi)^{1/2} \sigma^l} \exp\left[-\frac{1}{2(\sigma^l)^2} \left\{y_i - \mu^l - \sum_{j \in \mathcal{N}_i} \beta_{ij}^l (y_j - \mu^l)\right\}^2\right]. \quad (3)$$

In the following two equations, we state the pixelwise and pairwise (clique sizes 1 and 2) potential functions of this SAR model to interpret how they act on pixel values within a neighborhood.

$$E^s(y_i) = \frac{(y_i - \mu^l)^2}{2(\sigma^l)^2}, \quad (4)$$

$$E^s(y_i, y_j) = (\beta_{ij}^l)^2 \frac{(y_i - \mu^l)(y_j - \mu^l)}{2(\sigma^l)^2}. \quad (5)$$

The pointwise potential function $E^s(y_i)$ penalizes large difference between pixel values and their mean. Weighted by β_{ij}^l values, the pairwise potential $E^s(y_i, y_j)$ penalizes the discrepancy in intensity deviation from corresponding mean in neighboring pixels. The pairwise energy will be minimum when both the neighboring pixels have low deviation.

More sophisticated models of [17] [14] are rich and therefore are expected to describe the pattern more accurately. However, they also require complicated learning and inference algorithms that are approximate and computationally expensive. As we will see in the results section, the simpler SAR model described in this section is capable of producing high detection ratios on different IR experiments.

3.2 MRF for Prior

The prior distribution $p(\mathbf{x})$ of labels is modeled by an Auto-Logistic MRF. The potential functions for Auto-Logistic model are as follows.

$$E^a(x_i) = \nu_i x_i, \tag{6}$$

$$E^a(x_i, x_j) = \gamma_{ij} x_i x_j. \tag{7}$$

Clearly, the pointwise potential function $E^a(x_i)$ grows with the number of pixels labeled as target class. The pairwise potential function $E^a(x_i, x_j)$ accumulates a certain value γ_{ij} whenever the neighboring pixel labels x_i and x_j both belong to the target class (recall $x_i \in \{0, 1\}$). This is illustrated in Figure 3 which demonstrates how changing the pixel label to 1 (target) increases clique cost. Auto-logistic MRF model tends to generate less detection while maintaining the label similarity in nearby pixels. This model is particularly suitable for target detection because typically targets are sparse and consume a small area in the image.

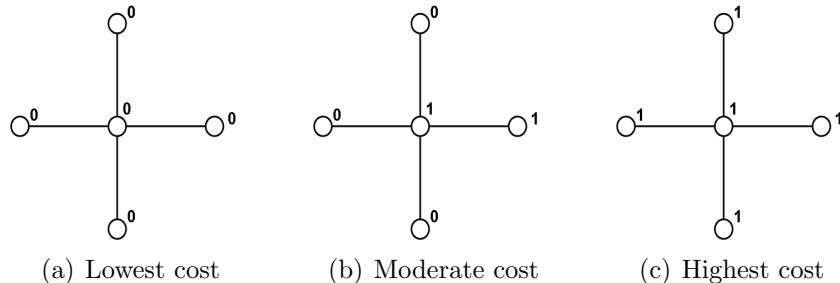


Figure 3: Example labeling of a pixel and its neighbors in a 4-way connectivity. The lowest cost is incurred when the pixel and all its neighbors are labels as 0 (background), as shown in leftmost figure. Auto model cost increases as more pixels are labeled as targets.

The conditional probability of any label x_i is given by

$$p(x_i | x_{\mathcal{N}_i}) = \frac{\exp[\nu_i x_i + \sum_{j \in \mathcal{N}_i} \gamma_{ij} x_i x_j]}{1 + \exp[\nu_i + \sum_{j \in \mathcal{N}_i} \gamma_{ij} x_j]}. \tag{8}$$

4 Parameter Estimation

The parameters of SAR and Auto-Logistic models are learned from labeled examples. The intensity mean for target and background pixels are estimated from labeled pixels for both classes. Since SAR model is defined by a set of equations in the form of Equation 2 [13], the linear coefficients β_{ij} and noise variances σ^2 are learned by Least Squares Linear Regression.

The parameters of the Auto-Logistic model was computed by the Pseudo-Likelihood (PLL) method. The product of all locally conditional probabilities is defined as the Pseudo-Likelihood in MRF literature.

$$pll(x) = \prod_i p(x_i | x_{\mathcal{N}_i}). \quad (9)$$

PLL is considered to be an approximation of the likelihood values for estimation purposes [13]. We applied a non-linear programming algorithm to maximize the log PLL of Auto-Logistic model, as stated below, in terms of the parameters.

$$lpll(x) = \sum_i \left\{ \nu_i x_i + \sum_{j \in \mathcal{N}_i} \gamma_{ij} x_i x_j \right\} - \sum_i \log \left\{ 1 + \exp(\nu_i + \sum_j \gamma_{ij} x_j) \right\}. \quad (10)$$

In all our experiments, the nonlinear optimization technique steadily converged to a solution in 15 ~ 20 iterations.

5 Inference

The optimal label configuration \mathbf{x}^* is computed by Iterated Conditional Mode (ICM) technique [2] for the proposed algorithm. The ICM algorithm works locally by determining the optimal label at each location given the observations and labels of its neighbors. In our scenario, the conditional probability to maximize at each location is proportional to the following:

$$p(y_i | x_i, y_{\mathcal{N}_i}) p(x_i | x_{\mathcal{N}_i}). \quad (11)$$

This is a product of conditional probabilities of pixel value and its label given those of its neighbors that are modeled by SAR and Auto-Logistic models (Equations 3 and 8) respectively. The labels are updated by $x_i^* =$

$\arg \max_x p(y_i | x_i, y_{N_i}) p(x_i | x_{N_i})$ iteratively until convergence. Several update schemes have been suggested for ICM in the literature. In our experiments, we updated the pixel locations and its neighbors (4-way connection) alternatively. This can be achieved by updating the alternate pixel in both horizontal and vertical directions for a 4-connectivity neighborhood [2].

It is important to clarify here that, the purpose of inference in our algorithm is to find the optimal label configuration \mathbf{x}^* and *not* to reconstruct or denoise the image by producing the optimal intensities at each location. The SAR MRF model is utilized solely to calculate the conditional probabilities.

6 Incorporating Temporal Information

In a video or temporally contiguous IR images sequence, the pattern of background intensity values of each image location can be statistically modeled by background subtraction techniques. In an attempt to reduce the amount of false positives, we combine the output of the coupled MRF (SAR-Auto) framework with that of a background subtraction method. To this end, we adopt the nonparametric statistical model proposed in [9]. This nonparametric method models the distribution of each pixel value over a certain period of time through Kernel Density Estimation (KDE) and computes a likelihood value for each pixel to belong to the background class. This probability is then checked against a threshold to generate the 0-1 decisions. Formally, let x_i^t be the intensity value at location i at time t . The probability of pixel i to be a background location given T previous observations x_i^t , $t = 1, \dots, T$, is computed by KDE by the following formula.

$$p(i \in \text{bckgnd}) \propto \frac{1}{T} \sum_{t=1}^T \exp \left[\frac{-1}{2\sigma^2} (x_i - x_i^t)^2 \right] \quad (12)$$

In this equation, the value of length of history T and kernel bandwidth σ are two external parameters. The value of $p(i \in \text{bckgnd})$ is discretized by a low threshold in order to minimize the false negative rate. The output of the coupled MRF model (or its variants, as explained later in experiments section) and the background subtraction are combined by a logical AND operations. Although more involved fusion strategy could be performed in this step (and we encourage the reader to do so whenever necessary), we found in our experiments that a logical AND is sufficient to produce a high detection rate with very few or no false positives.

7 Experimental Results

We tested our method on three datasets of OTCBVS benchmark data [1] : Dataset 01 and 03 with IR images of people walking on the street and Dataset 05 with two divers coming out of the water (referred to as IRD01, IRD03 and IRD05 resp.). IRD01 contains 261 IR images in 9 subsets (excluding Subset 3 which contains inverse IR images) with relatively darker (colder) background regions, see Figure 1 (a) and (d) for sample images. However, the brightness of targets also vary significantly among different sequences, notably in Subsets 7, 9, 10. On the other hand, the images in IRD03 and IRD04 (image sets 5a and 4a in Dataset 03 of OTCBVS) consists of images with brighter target and background regions as shown in Figure 1 (b) and (e).

IRD05 is particularly interesting for detection IR images since the targets in this dataset are so called ‘cold’ targets. That is, the temperature of the two divers in these images are too low for the IR camera to mark them with bright pixels (Figure 1(c), (f)). As a result, pixels on the target appear to be very similar to those in the background.

For IRD01, IRD03 and IRD04, the parameters were learned from 50, 100 and 100 randomly selected images respectively. Due to scarcity of targets in IR03, more images were necessary to gather enough observation for learning. In IRD05 images, we learn the models from 50 images where only one target is visible and test the method on 70 images where both the targets are visible. Sample training and test images of IRD05 are shown in Figure 4.

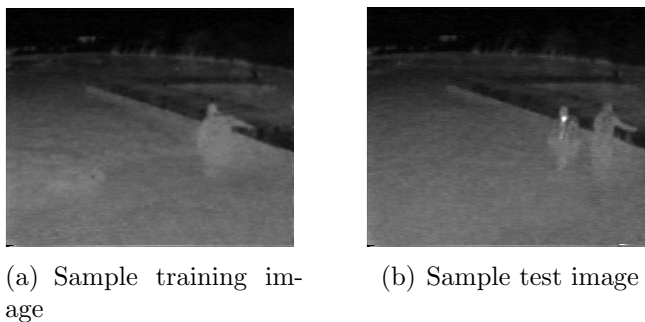


Figure 4: Sample training and test image for IRD05.

The pixel intensities within the target bounding boxes are utilized to es-

estimate the parameters of target SAR model. For background SAR model, we randomly selected background patches of same size as targets and used pixels within for learning. Figure 5(a) shows an image with target (solid) and background (yellow dashed) bounding boxes overlaid on it. The neighborhood used for both SAR and Auto-Logistic model is the 4-way associativity as shown in Figure 5(b). In intensity SAR model, each of the four connections are regarded as cliques and will be associated with different mixing weights β_{ij}^l . The Auto-Logistic model on labels was simplified by constraining the γ_{ij} values for four neighbors to be the same.

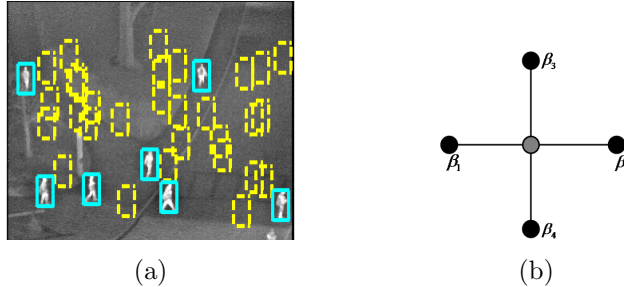


Figure 5: (a) Bounding boxes around target and background regions. (b) Four way connectivity.

The built in generic solvers for linear regression and nonlinear optimization problems on Matlab were used for parameter estimation of SAR and Auto-logistic models respectively. Learning the models required less than 5 minutes for all the datasets on an Intel Pentium 1.83GHz PC with 1 GB RAM. During inference, a mex-C++ implementation of ICM converged to optimal labeling within 15 iterations and required approx 1 second per frame on average.

To retrieve the target location from the output of ICM, we utilized the ratio of conditional probability values $\rho_i = \frac{p(y_i | 1, y_{N_i}) p(1 | x_{N_i})}{p(y_i | 0, y_{N_i}) p(0 | x_{N_i})}$ each pixel i . These values are thresholded at several different level δ_k , $k = 1, \dots, K$. Pixels with $\rho_i > \delta_k$ are congregated by a connected component search and the center of each connected component is considered to be the candidate locations. The number of detections is further reduced by merging overlapping boxes. Bounding boxes with 50% overlap are merged together and the mean of their centers become the center of the new detected location. Every detected location having a 30% overlap with a groundtruth target bounding box is

counted as a correct detection for performance evaluation.

In order to compare the contribution of each of the intensity (SAR) and label (Auto-Logistic) MRF models, we experimented with two other simplified methods on these datasets as follows.

1. SAR-i model: represents the conditional probability $p(\mathbf{y} \mid \mathbf{x})$ using SAR model but assumes the labels to be independent of each other. The probability of each label to be 1 (i.e., each pixel to be a target pixel) is computed empirically from training data.
2. i-Auto model: considers the intensities to be iid Gaussian and models the the prior $p(\mathbf{x})$ using Auto-Logistic MRF. The parameters for Gaussian model for intensity are computed empirically from training data.

That is, SAR-i and i-Auto assume independence in one of the two layers that the proposed method considers to be dependent. The Bayesian networks for these two models are illustrated in Figure 6.

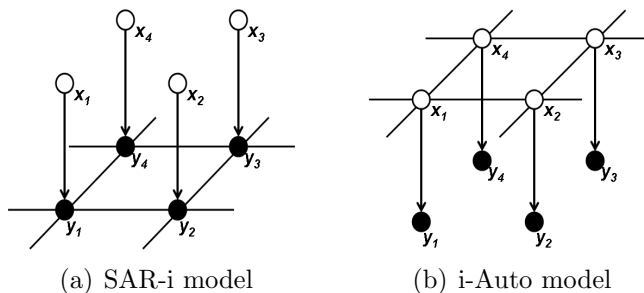


Figure 6: Bayesian networks for SAR-i and i-Auto.

The performance comparison of these methods are shown in Figure 7 where SAR-Auto refers to the proposed method. The proposed method clearly exhibit a better performances than both SAR-i and i-Auto methods for all datasets.

It is evident from the ROC curves that the proposed method SAR-Auto achieves a high rate of detection, especially with FA rate ≤ 1 per frame. However, in IRD03 and IRD04, we observe occurrence of many patches that has a high resemblance in intensity pattern with target patches. That is why the proposed algorithm generates higher rate of false alarms for IRD03

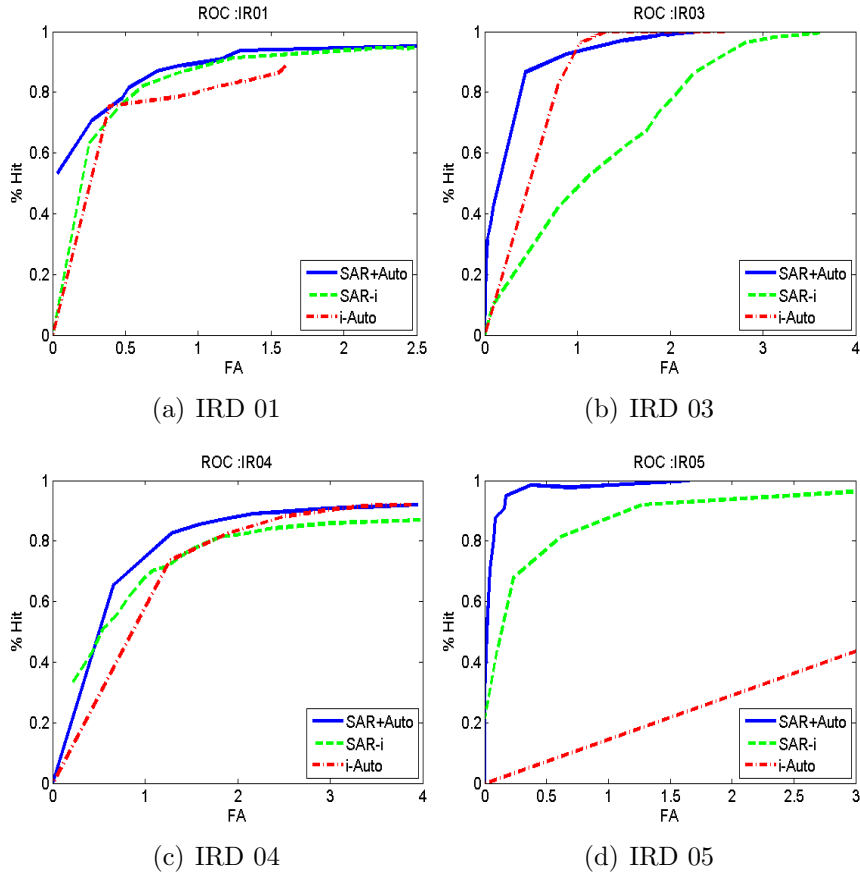


Figure 7: ROC curves of proposed (SAR-Auto, in blue solid) and SAR-i (red dotted), i-Auto (green dashed) methods.

and IRD04. It is interesting to observe that targets in these two image collections are significantly brighter than the surrounding background. As a result, the i-Auto model exhibits similar HIT and FA values of the coupled SAR-Auto, i.e., pixelwise intensities independently are capable of producing good detection rates.

In datasets IRD01 and IRD05, the pixel intensities at individual locations do not vary much between target and background classes. However, the pattern of intensity arrangement within an image patch is substantially different in these two classes. The i-Auto approach, which models the intensities independently, generates many incorrect detections in both IRD 01 and 05. On

the other hand, the SAR-i approach, which models the intensity correlation within the image patch, performs better than i-Auto on these datasets. These results suggest one needs to model both the label and intensity dependence pattern in order to be robustly detect targets in varying IR scenes. Sample qualitative results are compared in Figure 8. These outputs were generated by operating at a false positive rate approximately 1 per frame for all three techniques.

7.1 Learned Parameters

We display the parameter values learned for SAR-Auto model – i.e., for SAR models of both target and background intensities and the Auto-Logistic model of labels – learned from IRD05 dataset. The left and right columns of Figure 9 displays the parameters of the SAR models for target and background respectively. The linear coefficients β_{ij}^l for each clique is shown above the dotted line in matrix form and the mean and variances $\mu^l, (\sigma^l)^2$ are shown below. The neighborhood relationship for background pixels (right column) are almost symmetric in horizontal and vertical directions indicating similar relationship between two neighbors in both both x and y-axis. On the other hand, β_{ij}^l for target is more informative as they are asymmetric in both directions. The parameters ν_i and γ_{ij} learned for this dataset are 9.54 and -4.6924 respectively (recall γ_{ij} values are constrained to be the same).

7.2 Incorporating background subtraction output

Adding temporal information through background subtraction was applied to datasets IRD 03 and IRD 04 both of which contain temporally contiguous frames. As stated before, the output of the MRF model outputs are combined with that of the background subtraction algorithm by a logical AND operation. We found this simple operation performs well and reduces most of the false positives. This is because (as is also elaborated at the end of this section with an example), the false positives of the MRF model and the background subtraction are almost always non-overlapping. We used the implementation of [9] provided by the author and selected the parameters of both the MRF and background subtraction models to minimize the false negatives as much as possible.

The output of each of the i-Auto, SAR-i and SAR-Auto (Figure 10(b)) approaches are combined with background subtraction result (Figure 10(c))

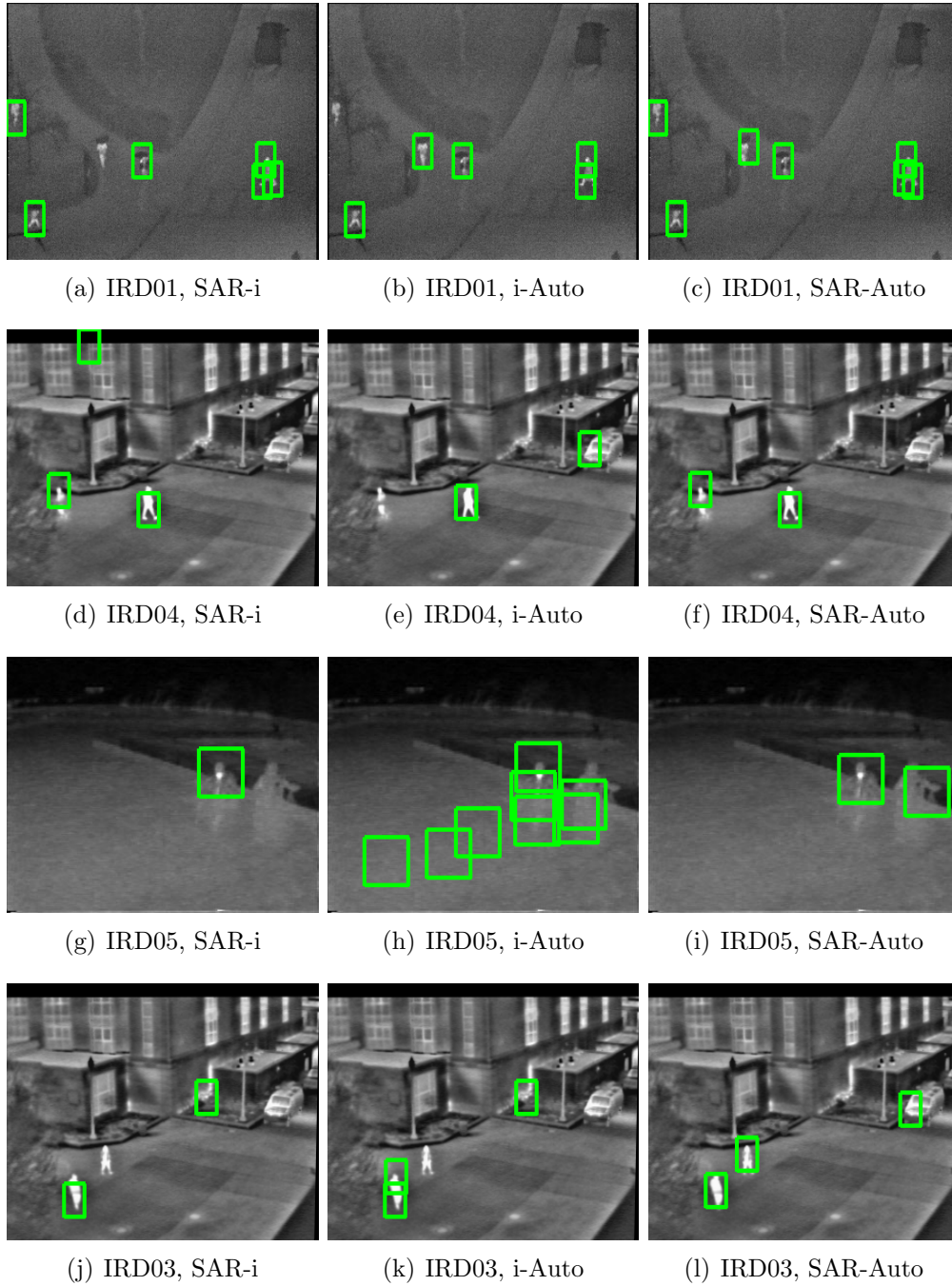


Figure 8: Sample input images for IR target detection.

$$\begin{array}{ccc}
\left[\begin{array}{cc} 0.044 & \\ 0.443 & 0.479 \\ & 0.068 \end{array} \right] & & \left[\begin{array}{cc} 0.016 & \\ 0.487 & 0.483 \\ & 0.016 \end{array} \right] \\
\text{.....} & & \text{.....} \\
117.4, 2.11 & & 86.53, 1.19
\end{array}$$

Figure 9: Learned parameters of SAR and Auto models.

with a pixelwise AND operator to generate the final output as shown in Figure 10(d). The numerical results of this process is reported in Table 1. For both the datasets, the table shows, from left to right, the average percentage of true positive and number of false positive per frame of [9] alone (with parameter tuned to achieve 0 false negative rate), those of each of the three aforementioned methods after adding background subtraction (HIT-a, FA-a) and the average FA rate (FA-b) corresponding to same detection accuracy without background subtraction. Incorporation of background subtraction information enables all three techniques to attain the largest possible true positive rate with zero false alarm.

Dataset	BGsub [9]		SAR-Auto		i-Auto		SAR-i	
	HIT	FA	HIT-a	FA-b → FA-a	HIT-a	FA-b → FA-a	HIT-a	FA-b → FA-a
IRD03	100	15.57	100	3.3 → 0	100	1.5 → 0	99.73	3.6467 → 0
IRD04	99.77	11.4	92.12	3.94 → 0	92.1	3.87 → 0	82.12	8.55 → 0

Table 1: Performance improvement with background subtraction.

There is an intuitive explanation why a logical AND operation between combination of the proposed method (e.g., SAR-Auto) and background subtraction results would remove the false positives. The SAR-Auto method generates false positives in the background regions that resembles the target pattern, and the intensities within does not change significantly i.e., typically static regions, for a period of time (shown in red in Figure 11). Background subtraction methods, by construction, would identify these regions as background. Therefore, the false detections from MRF models and the background subtraction method generally do not overlap with each other.

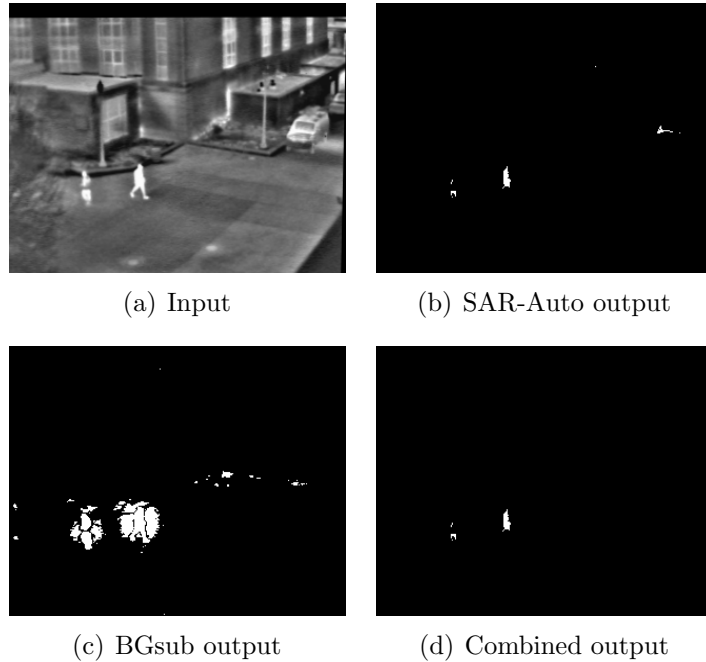


Figure 10: Combining background subtraction with SAR-Auto.

8 Conclusion

This study demonstrates the advantage of enforcing neighborhood dependence in both intensity and label layers for IR target detection. The intensity and label value at any pixel is related to those of its neighbors by SAR and Auto-Logistic MRF models respectively. High accuracies achieved in our experiments suggest these models were able to learn the local image patterns adequately enough for locating object regions in IR image. We show that independence assumption in any of the two layers (intensity and label) would deteriorate the performance, i.e., coupling two MRF models with each other is necessary for satisfactory performance. Furthermore, we combine temporal information into the framework to improve the detection accuracy. We strongly believe findings in this paper will provide new insight and instigate research in utilizing patch appearance and the dependence among the pixels within for target detection in infra-red imagery.



Figure 11: Sample false positives (red boxes) of SAR-Auto.

References

- [1] OTCBVS benchmark dataset. <http://www.cse.ohio-state.edu/otcbvs-bench/>.
- [2] J. Besag. On the statistical analysis of dirty pictures. *Journal of Royal Statistical Society*, 48(3), 1986.
- [3] B. Leibe, A. Leonardis, and B. Schiele. Robust object detection with interleaved categorization and segmentation. *IJCV*, 77:259–289, 2008.
- [4] Yuri Y. Boykov and Marie-Pierre Jolly. Interactive graph cuts for optimal boundary and region segmentation of objects in n-d images. In *ICCV*, 2001.
- [5] Congxia Dai, Yunfei Zheng, and Xin Li. Layered representation for pedestrian detection and tracking in infrared imagery. In *CVPR Workshop OTCBVS*, 2005.
- [6] N. Dalal and B. Triggs. Histograms of oriented gradients for human detection. In *CVPR*, 2005.
- [7] James W. Davis and Vinay Sharma. Robust background-subtraction for person detection in thermal imagery. In *CVPR Workshop OTCBVS*, 2004.
- [8] Haluk Derin and William S Cole. Segmentation of textured images using gibbs random fields. *Computer Vision, Graphics and Image Processing*, 35:72–98, July 1986.

- [9] Ahmed M. Elgammal, David Harwood, and Larry S. Davis. Non-parametric model for background subtraction. In *ECCV*, 2000.
- [10] Kai Jungling and Michael Arens. Feature based person detection beyond the visible spectrum. In *CVPR Workshop OTCBVS*, 2009.
- [11] M. Pawan Kumar, Philip H. S. Torr, and A. Zisserman. Obj cut. In *CVPR*, 2005.
- [12] Alex Leykin and Riad Hammoud. Robust multi-pedestrian tracking in thermal-visible surveillance videos. In *CVPR Workshop OTCBVS*, 2006.
- [13] Stan Z. Li. *Markov Random Field Modeling in Image Analysis (Advances in Pattern Recognition)*. Springer, 2001.
- [14] B. S. Manjunath, T. Simchony, and R. Chellappa. Stochastic and deterministic networks for texture segmentation. *IEEE Trans. on Acoustic, Speech and Signal Processing*, 38, June 1990.
- [15] T. Parag, A. Elgammal, and A. Mittal. A framework for feature selection for background subtraction. In *CVPR*, 2006.
- [16] Toufiq Parag. Coupled label and intensity mrf models for ir target detection. In *CVPR Workshop OTCBVS*, 2011.
- [17] Stefan Roth and Michael J. Black. Fields of experts: A framework for learning image priors. In *CVPR*, 2005.
- [18] C. Rother, V. Kolmogorov, and A. Blake. Grabcut: Interactive foreground extraction using iterated graph cuts. In *ACM Transactions on Graphics (SIGGRAPH'04)*, 2004.
- [19] Tal Simchony and Rama Chellappa. Stochastic and deterministic algorithms for map texture segmentation. In *International Conference on Acoustics, Speech, and Signal Processing*, 1988.
- [20] Lorenzo Torresani, Vladimir Kolmogorov, and Carsten Rother. Feature correspondence via graph matching: Models and global optimization. In *ECCV*, 2008.

- [21] Vijay Venkataraman and Fatih Porikli. Relcom: Relational combinatorial features for rapid object detection. In *CVPR Workshop OTCBVS*, 2010.
- [22] P. Viola, M. Jones, and D. Snow. Detecting pedestrians using patterns of motion and appearance. In *ICCV*, 2003.
- [23] Junxian Wang, George Bebis, and Ronald Miller. Robust video-based surveillance by integrating target detection with tracking. In *CVPR Workshop OTCBVS*, 2006.
- [24] R. Zabih and V. Kolmogorov. Spatially coherent clustering with graph cuts. In *CVPR*, 2004.
- [25] Li Zhang, Bo Wu, and Ram Nevatia. Pedestrian detection in infrared images based on local shape features. In *CVPR Workshop OTCBVS*, 2007.